Throughput maximization through Network-Based Stream-Number Decision for MIMO HSDPA

Govinda Lilley, Martin Wrulich and Markus Rupp
Institute of Communications and RF Engineering, Vienna University of Technology
{glilley,mwrulich,mrupp}@nt.tuwien.ac.at

***Abstract*—3GPP standardized double-stream transmit antenna array (D-TxAA) in Release 7 as the successor of classical single-input single-output (SISO) HSDPA, supporting a maximum of 42.2 Mbit/s [1]. To achieve these high throughputs, the number of parallel streams that are utilized during a transmission time interval (TTI) should be chosen to suit the current channel conditions. Thus, either the mobile or the network (NodeB) has to derive a decision upon the stream-utilization based on this information. Although the standard permits the evaluation of the number of streams on the mobile (and signaling it to the NodeB), the necessary SINR estimation for both the single- and double-stream case is difficult. Furthermore, the network operator may opt to have the number of streams being decided in the NodeB to keep control of the spatial interference structure in the cell. In this paper, we introduce two network-based stream decision algorithms and investigate them by means of system-level simulations to compare their performance to the mobile-based stream number decision.**

I. Introduction

During the last years, high-speed downlink packet access (HSDPA) has led to a significant increase in mobile data usage, and the throughput demand in modern communication systems is expected to grow even faster in the next years. In order to satisfy this demand, 3GPP standardized a successor of the WCDMA-based single-input single-output HSDPA that supports multiple antennas on both the transmitter and the receiver side.

As part of the 3GPP Release 7 [2], double-stream transmit antenna array (D-TxAA) has been defined as the transmission scheme for multiple-input multiple-output (MIMO) HSDPA communication. This scheme allows for the parallel transmission of up to two independent data streams, supporting a theoretical maximum data rate of 42.2 Mbit/s [1], [3]. The next generation communication system—Long Term Evolution (LTE)—will even outperform this limit [4], [5]. However, these networks need a completely new wireless infrastructure, and accordingly network operators will most probably introduce MIMO HSDPA before going towards LTE.

The D-TxAA scheme or Release 7 HSDPA relies on the parallel transmission of two data streams, where the number of utilized streams depends on the current channel conditions, similar to the concept of adaptive modulation and coding (AMC). The standard [2] does not fully specify the feedback scheme, but given the basic requirements it permits the evaluation and signaling of the number of streams from the mobile side. Typically such an evaluation would be based on a suitable SINR estimation [6].

Such an estimation depends on a number of factors and can be very challenging [7], [8]. In addition, the interference structure in the cell - a factor that depends on the number of active streams - is determined by by the equipment, which in general is undesired by the network operators [9]. Individual enhancements of the user channel quality by means of interference-canceling [10], [11] or similar techniques do not impose such problems. Still, for an efficient network operation, network entities should assign the resources according to overall goals, e.g. the average cell-throughput [12]–[14], and therefore actively manage the interference situation in the cells.

In this paper we introduce two different (*network-based*) stream number decision algorithms that are based upon the CQI and ACK/NACK reports of the user equipment. We compare the performance of our algorithms with the performance of the user-based stream number decision where full CSI is available. Furthermore, the necessary thresholds of the algorithms are evaluated by system-level simulations [15] to identify the optimum operation points.

The paper is organized as follows: Section II explains the system-level modeling and some details about our simulator. Section III and IV introduce the reference and network-based stream decision algorithms, with their performance being evaluated in Section V. Finally, we conclude the paper in Section VI.

II. System Model and Simulator Details

To assess the performance of the proposed algorithms, we utilized a MIMO HSDPA system level simulator [16], developed in a MATLAB-environment. The simulator can basically be split in three different parts, (1) channel quality evaluation, (2) performance prediction (i.e. BLER evaluation), and (3) network/user handling including all relevant algorithms, depicted in Figure 1. It has to be noted that the channel quality evaluation relies on the utilization of so-called *fading-parameters* that account for a computationally efficient evaluation [15].

The system-level simulator allows for the investigation of MIMO HSDPA networks in terms of block error rates, throughput, scheduler performance and other network-related performance measures. The investigated networks are of 3GPP type one layout [17] but can be configured in terms of simulated users, timing, interference structure, size and many more. Besides the physical layer abstraction, all layer-functionalities

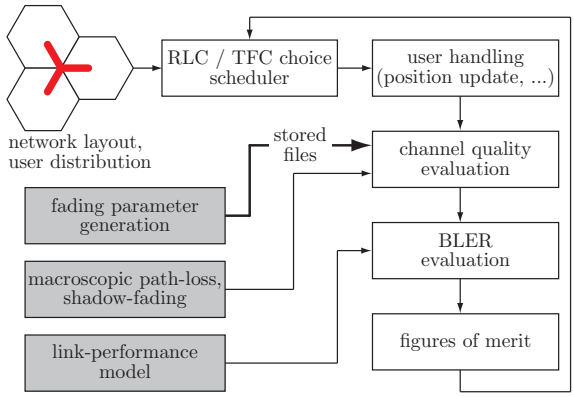

Fig. 1. Overview of D-TxAA MIMO HSDPA system level simulator [16]. The functionality can be split in three main parts, (1) channel quality evaluation, (2) performance prediction, and (3) network/user handling.

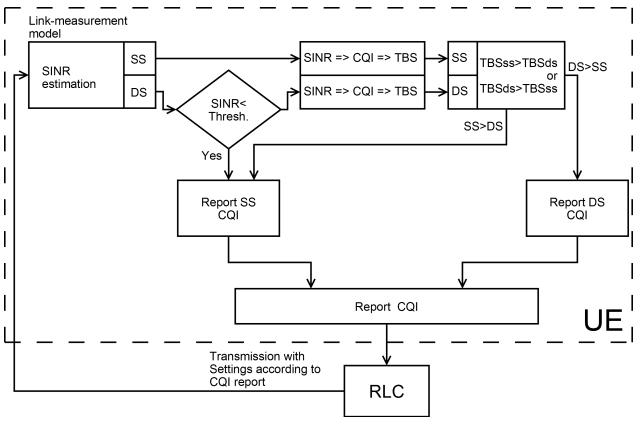

Fig. 2. UE Stream-Number Decision algorithm.

up to the MAC-d are implemented, with a special focus on MAC-hs algorithms, i.e. scheduling and physical layer resource management.

III. User Equipment Stream Decision Algorithm

The User Equipment (UE) Stream Decision algorithm is based on the fact that the UE has quasi full channel state information (CSI) and hence should be able to calculate the optimal transmission settings. Therefore this algorithm will be used as a reference to which our other algorithms shall be compared. The algorithm is shown in Figure 2.

The UE calculates the SINR for single stream (SS) and double stream (DS) transmission scenarios. As long as the SINR of stream 2 in DS transmission mode $\text{SINR}_{\text{DS},2}$ is above the threshold $\text{SINR}_{thr.}$, the UE is allowed to decide how many streams to use. If the UE is permitted a decision and the double stream transport block size TBS_{DS} is greater than the single stream transport block size TBS_{SS}, two streams are used. In all other cases the transmission is single-streamed. Note that TBS = TBS(CQI(SINR)) where the mapping CQI(SINR) is extracted from AWGN link level simulations. Essentially the stream number decision is given by

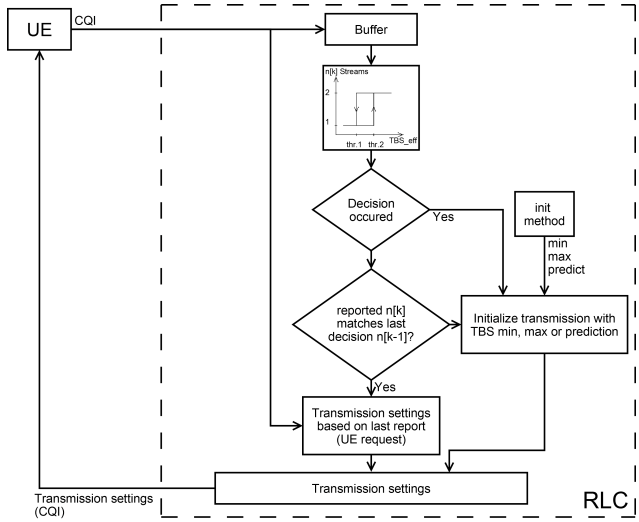

Fig. 3. RLC Stream-Number Decision algorithm based on CQI reports.

$$n_k = \begin{cases} 1, & \text{if } \text{SINR}_{\text{DS},2} < \text{SINR}_{thr.} \vee \text{TBS}_{\text{DS}} < \text{TBS}_{\text{SS}} \\ 2, & \text{if } \text{SINR}_{\text{DS},2} \geq \text{SINR}_{thr.} \wedge \text{TBS}_{\text{DS}} \geq \text{TBS}_{\text{SS}}. \end{cases} \quad (1)$$

After the stream number decision has been made, the CQI corresponding to the decision is reported to the radio link control (RLC), which then uses the transmission settings associated with it for the next transmission.

IV. Radio Link Control Stream Decision Algorithms

Signal processing in handheld devices is usually constrained in complexity due to limited battery capacity. Thus, if a user-based stream number decision were to be implemented, it would consume even more computational resources and battery. The network operator also has less control over the spatial interference situation, which is influenced by the number of used streams and their precoding. Furthermore, advanced schedulers utilizing the number of streams as an optimization parameter are rendered impossible. These issues do not exist when the stream number decision is moved to the RLC. We propose two algorithms, with the first one using only CQI reports from the UE to calculate the optimal transmission settings. The second algorithm uses a combination of CQI and ACK/NACK reports for transmission settings computation in order to optimize the BLER.

Figure 3 shows our first RLC Stream Decision algorithm which bases its decision on the CQI report history of the UE. The reports are saved in up- and downgrade FIFO buffers of lengths N_u and N_d, respectively. These reports are converted to corresponding TBS values, which are then compared to up- and downgrade thresholds in order to decide how many streams will be used. The stream number decision is given by

$$n_k = \begin{cases} 1, & \text{if TBS}_i(\text{CQI}_i) < \text{TBS}(\text{CQI}_d),\ i = 1...N_d \\ 2, & \text{if TBS}_j(\text{CQI}_j) > \text{TBS}(\text{CQI}_u),\ j = 1...N_u \\ n_{k-1}, & \text{otherwise,} \end{cases} \tag{2}$$

where CQI_i is taken from the downgrade FIFO buffer, CQI_j is taken from the upgrade buffer and k represents the current TTI index. $\text{TBS}(\text{CQI}_d)$ and $\text{TBS}(\text{CQI}_u)$ are the down- and upgrade thresholds which we generate from CQI thresholds. Since the CQI to TBS mapping is unique and CQIs are the same for all mapping tables, using CQIs rather than TBS values as thresholds is practical.

After up- or downgrading, the transmission settings that will be utilized have to be determined. We implemented three initialization methods in order to compare their impact on throughput performance and ACK/NACK ratio. For the first two methods the CQI is set to either the maximum or the minimum CQI value available within the selected CQI mapping table (e.g. 30 or 1 for single stream). The third method is based on extrapolation of TBS values via linear least square approximation. The TBS values are extracted from the CQI reports within the upgrade buffer, because this buffer contains the most recent reports and hence will deliver a more accurate prediction. In case of a downgrade, the predicted TBS value TBS_P is directly used to calculate the transmission settings. In case of an upgrade, TBS_P is distributed over both streams where $\text{TBS}_{stream1} = \alpha \cdot \text{TBS}_P$ and $\text{TBS}_{stream2} = (1-\alpha) \cdot \text{TBS}_P$ are the TBS values for stream 1 and 2, respectively, and α is the distribution factor. $\text{TBS}_{stream1}$ and $\text{TBS}_{stream2}$ are then used to gain the transmission settings for stream 1 and 2. In an effort to keep complexity low, α is kept constant and computed as follows

$$\alpha = \frac{\text{TBS}(\text{CQI}_1)}{\text{TBS}(\text{CQI}_1) + \text{TBS}(\text{CQI}_1 - \Delta\text{CQI})} \tag{3}$$

$\text{TBS}(\text{CQI}_1)$ is the TBS of the first stream, and $\text{TBS}(\text{CQI}_1 - \Delta\text{CQI})$ represents the TBS of the second stream, which in average is ΔCQI lower than the first due to the precoding favouring stream 1, see [15]. Note that the precoding is optimised for stream 1 consequently resulting in a higher BLER for stream 2. To find an appropriate value for ΔCQI we ran a simulation of our UE sided (reference) algorithm. The CQI trace of the simulation and average CQIs are shown in Figure 4 and a plot of α over CQI_1 is shown in Figure 5. The mapping TBS(CQI) is done according to [2].

It is also important to note, that immediately after an up- or downgrade decision, due to the feedback delay, no reports of the UE for the current stream number decision are available. Accordingly, the RLC transmits with the new transmission settings until valid reports have been recieved.

Our second algorithm is very similar to the first, save for the fact that the ACK/NACK ratio is also considered in order to improve the overall BLER, and that transmission initialization after an up- or downgrade is always done via linear least square extrapolation of the TBS weighted with the average BLER.

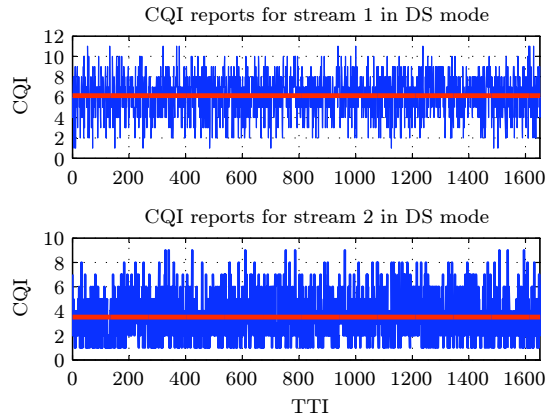

Fig. 4. CQI trace of a double stream transmission for the UE-based Stream-Number decision algorithm.

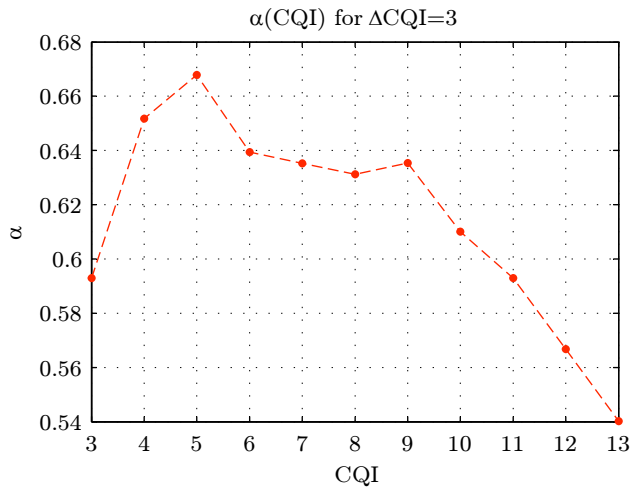

Fig. 5. α for CQI of the first stream for $\Delta\text{CQI} = 3$.

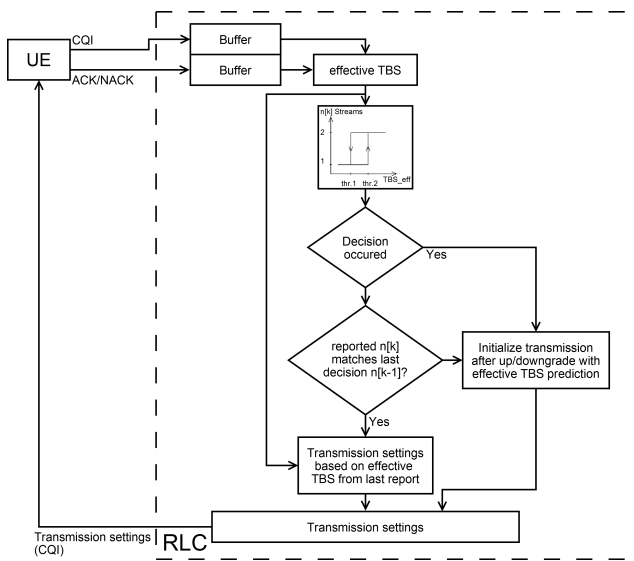

Fig. 6. RLC Stream-Number Decision algorithm based on effective TBS.

Figure 6 shows our second algorithm with the decision being expressed as

$$n_k = \begin{cases} 1, & \text{if } \mathrm{TBS}_{\mathrm{eff},i}(\mathrm{CQI}_i) < \mathrm{TBS}_{\mathrm{eff},d}(\mathrm{CQI}_d),\ i = 1...N_d \\ 2, & \text{if } \mathrm{TBS}_{\mathrm{eff},j}(\mathrm{CQI}_j) > \mathrm{TBS}_{\mathrm{eff},u}(\mathrm{CQI}_u),\ j = 1...N_u \\ n_{k-1}, & \text{otherwise,} \end{cases} \tag{4}$$

where the effective TBS of element i within the up/downgrade buffer $\mathrm{TBS}_{\mathrm{eff},i} = \mathrm{TBS}_i \cdot (1 - \mathrm{BLER})$ and BLER is the average of the most recent 40 ACK/NACK reports. The effective TBS threshold $\mathrm{TBS}_{\mathrm{eff},u/d}(\mathrm{CQI}_{u/d}) = \mathrm{TBS}_{u/d}(\mathrm{CQI}_{u/d}) \cdot (1 - \mathrm{BLER}_{\mathrm{target}})$ is the product of the TBS threshold and the desired overall transmission efficiency $(1 - \mathrm{BLER}_{\mathrm{target}})$ the system should have. In addition the transmitted TBS is reduced by the averaged ACK/NACK ratio to further decrease BLER. Note that as in the previous algorithm, after an up- or downgrade, the RLC transmits with the new transmission settings until valid reports are available.

V. Simulation Details

In this section we present simulation results for various thresholds of the algorithms discussed above and compare them to the performance of our reference algorithm. Noteworthy results can be expected for the up- and downgrade thresholds, which therefore will be covered here. In Figure 7, the average cell throughput is plotted for the TBS-based algorithm and an increasing downgrade threshold CQI_d. The low throughput at 0 and 1 results from an effective downgrade prevention caused by $\mathrm{TBS}(\mathrm{CQI}_{\mathrm{DS},0}) = \mathrm{TBS}(\mathrm{CQI}_{\mathrm{DS},1})$, where $\mathrm{TBS}(\mathrm{CQI}_j) > \mathrm{TBS}(\mathrm{CQI}_u)$ is always valid, thereby greatly increasing BLER, as can be seen in Figure 8. Splitting of the throughput and BLER curves for the three initialization methods, observed at downgrade thresholds greater than 2, is the result of a drastic reduction of DS transmissions due to the more aggressive downgrading. The low amount of DS transmissions coupled with most transmissions being downgraded shortly after being upgraded gives transmissions with optimized transmission initialization an obvious advantage, which can be seen in Figures 7 and 8. For the $\mathrm{TBS}_{\mathrm{eff}}$-based algorithm, the BLER is shown in Figure 9. The BLER is very close to the target value of 10% due to the feedback of transmission settings based on effective TBS. Since this algorithm keeps the BLER of stream 1 close to 10%, the benefit is a high throughput, even under suboptimal conditions. In a further simulation with a suboptimal mapping of $\mathrm{CQI}(\mathrm{SINR}_{\mathrm{opt.}}+1\mathrm{dB})$, we observed a maximum throughput gain of 650 kBit/s, which is depicted in Figure 10. This case is of particular interest, when the estimators necessary for evaluating the feedback in the UE do not work properly or are poorly implemented.

For a variable upgrade threshold CQI_u the results are shown in Figures 11 and 12. The simulations show an upward trend of the throughput, which is a result of the decreasing BLER associated with increasingly conservative upgrading. The effect of higher upgrade thresholds is shown in Figures 13 and 14.

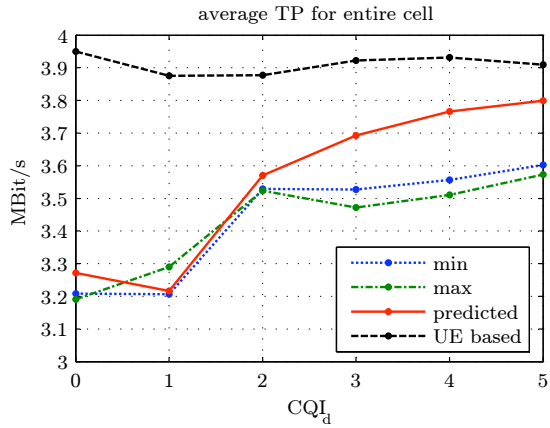

Fig. 7. Throughput simulation of the RLC-TBS-based algorithm for $\mathrm{CQI}_d = 0...5$.

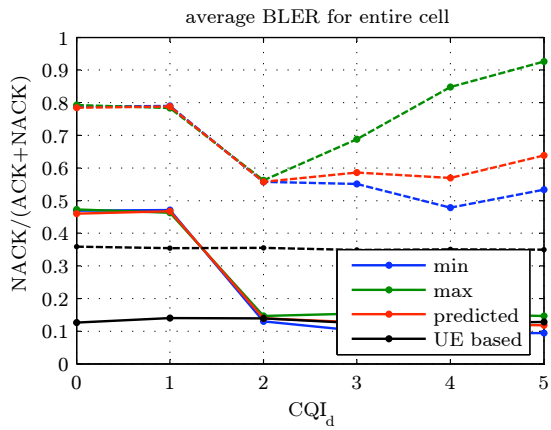

Fig. 8. Simulation results for the BLER of the RLC-TBS-based algorithm with $\mathrm{CQI}_d = 0...5$. Full lines represent stream 1 and dashed lines represent stream 2. The blue lines (min) are for initialization of the transmission with the minimum value, green lines (max) are for initialization with the maximum value, red (predicted) is for initialization based on linear least square extrapolation and black (UE-based) is the average BLER for the UE-based reference algorithm.

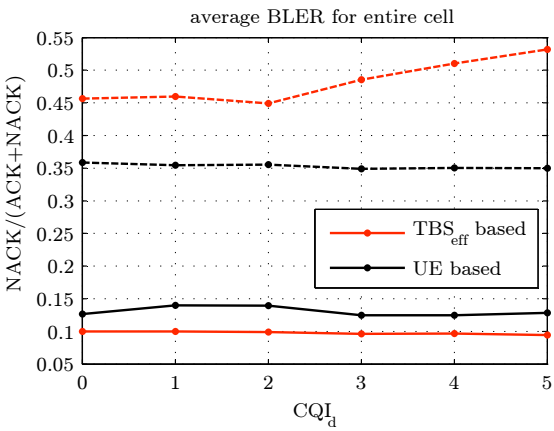

Fig. 9. Simulation results for the BLER of the RLC-$\mathrm{TBS}_{\mathrm{eff}}$-based algorithm with $\mathrm{CQI}_d = 0...5$. Full lines represent stream 1 and dashed lines represent stream 2.

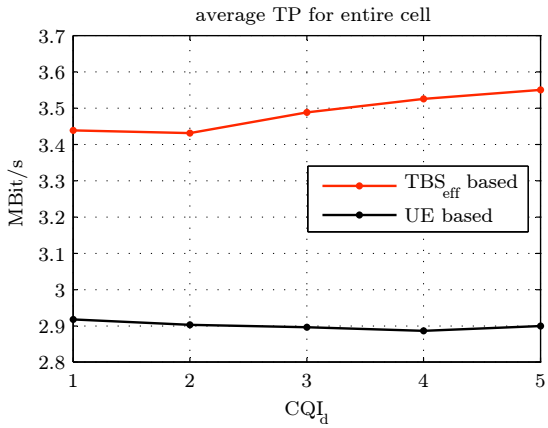

Fig. 10. Simulation results for the troughput of the RLC-TBS$_{\text{eff}}$-based algorithm with CQI$_d$ = 1...5 and suboptimal mapping of CQI(SINR$_{\text{opt.}}$ + 1dB).

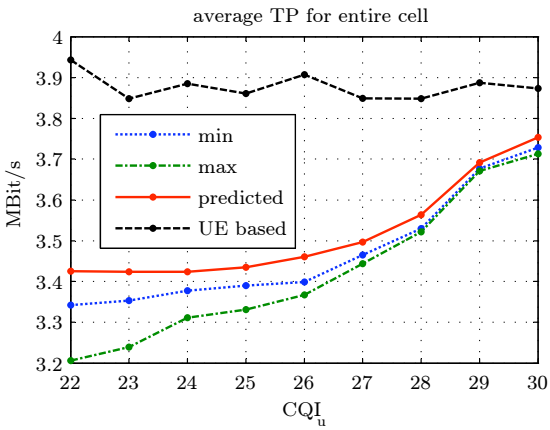

Fig. 11. Throughput results of the RLC-TBS-based algorithm with CQI$_u$ = 22...30.

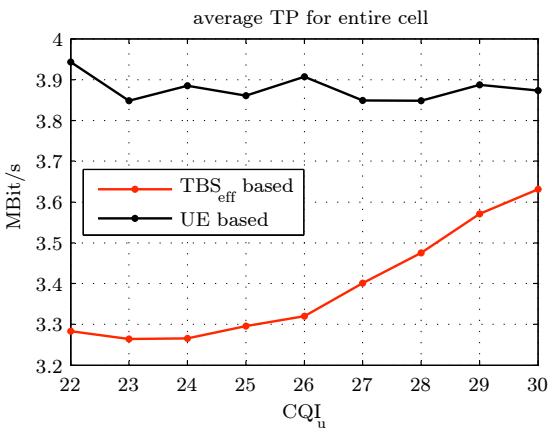

Fig. 12. Throughput results of the RLC-TBS$_{\text{eff}}$-based algorithm with CQI$_u$ = 22...30.

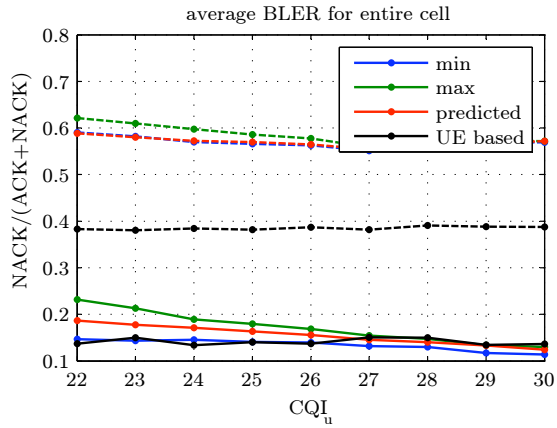

Fig. 13. Simulation results for the BLER of the RLC-TBS-based algorithm with CQI$_u$ = 22...30. Full lines represent stream 1 and dashed lines represent stream 2.

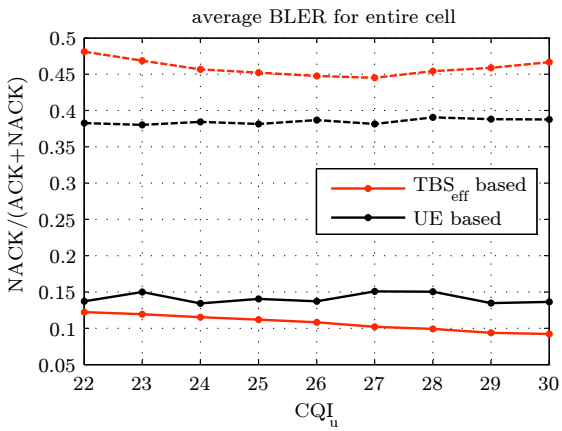

Fig. 14. Simulation results for the BLER of the RLC-TBS$_{\text{eff}}$-based algorithm with CQI$_u$ = 22...30. Full lines represent stream 1 and dashed lines represent stream 2.

VI. Conclusions

In this paper we discuss and investigate two RLC-based stream number decision algorithms and compare them to UE-based stream number decision performance. Simulations show good average throughput and BLER values for the TBS-based algorithm with linear least square predictive initialization at aggressive downgrade thresholds and low DS counts. Also downgrade blocking at downgrade thresholds CQI$_d$ of 0 and 1 was observed for the TBS-based algorithm, which lead to significant degradation of throughput performance. Finally we investigated the behaviour of our algorithms for suboptimal conditions. The TBS$_{\text{eff}}$-based algorithm proved to have the highest throughput, while retaining performance similar to the TBS-based algorithm under improved conditions. This case is particularly interesting when the estimators necessary for evaluating the feedback do not work properly or are poorly implemented.

ACKNOWLEDGMENT

This work has been funded by *mobilkom Austria AG* and the Institute of Communications and Radio-Frequency Engineering. The authors would like to thank C. Mehlführer for many fruitful discussions. The views expressed in this paper are those of the authors and do not necessarily reflect the views within *mobilkom Austria AG*.

REFERENCES

[1] T. Nihtila and V. Haikola, "HSDPA MIMO system performance in macro cell network," in *Proc. IEEE Sarnoff Symposium*, 2008, pp. 1–4.

[2] Members of 3GPP, "Technical specification group radio access network; physical layer procedures (FDD)," 3GPP, Tech. Rep. 3GTS 25.214 Version 7.4.0, Mar. 2007.

[3] H. Holma and A. Toskala, *HSDPA/HSUPA for UMTS: High Speed Radio Access for Mobile Communications*. John Wiley & Sons, Ltd., 2006, ISBN 0-470-01884-4.

[4] E. Dahlman, S. Parkvall, J. Skold, and P. Beming, *3G Evolution: HSDPA and LTE for Mobile Broadband*. Academic Press, Jul. 2007.

[5] C. Mehlführer, M. Wrulich, J. Colom Ikuno, D. Bosanska, and M. Rupp, "Simulating the long term evolution physical layer," submitted to EUSIPCO 2009.

[6] C. Mehlführer, S. Caban, M. Wrulich, and M. Rupp, "Joint throughput optimized CQI and precoding weight calculation for MIMO HSDPA," in *Proc. 42nd Asilomar Conference on Signals, Systems and Computers*, Oct. 2008.

[7] M. Wrulich and M. Rupp, "Efficient link measurement model for system level simulations of Alamouti encoded MIMO HSDPA transmissions," in *Proc. ITG International Workshop on Smart Antennas (WSA)*, Darmstadt, Germany, Feb. 2008.

[8] J. Colom Ikuno, M. Wrulich, and M. Rupp, "Performance and modeling of LTE H-ARQ," in *Proc. ITG International Workshop on Smart Antennas (WSA)*, Berlin, Germany, Feb. 2009.

[9] A. Mäder, D. Staehle, and M. Spahn, "Impact of HSDPA radio resource allocation schemes on the system performance of UMTS networks," in *Proc. IEEE 66th Vehicular Technology Conference Fall (VTC)*, 2007, pp. 315–319.

[10] M. Wrulich, C. Mehlführer, and M. Rupp, "Interference aware MMSE equalization for MIMO TxAA," in *Proc. IEEE 3rd International Symposium on Communications, Control and Signal Processing (ISCCSP)*, 2008, pp. 1585–1589.

[11] C. Mehlführer, M. Wrulich, and M. Rupp, "Intra-cell interference aware equalization for TxAA HSDPA," in *Proc. IEEE 3rd International Symposium on Wireless Pervasive Computing*, 2008, pp. 406–409.

[12] K. I. Pedersen, T. F. Lootsma, M. Stottrup, F. Frederiksen, T. Kolding, and P. E. Mogensen, "Network performance of mixed traffic on high speed downlink packet access and dedicated channels in WCDMA," in *Proc. IEEE 60th Vehicular Technology Conference (VTC)*, vol. 6, 2004, pp. 4496–4500.

[13] M. Wrulich, W. Weiler, and M.Rupp, "HSDPA performance in a mixed traffic network," in *Proc. IEEE Vehicular Technology Conference Spring (VTC)*, May 2008, pp. 2056–2060.

[14] H. Chao, Z. Liang, Y. Wang, and L. Gui, "A dynamic resource allocation method for HSDPA in WCDMA system," in *Proc. IEE International Conference on 3G Mobile Communication Technologies*, 2004, pp. 569–573.

[15] M. Wrulich, S. Eder, I. Viering, and M. Rupp, "Efficient link-to-system level model for MIMO HSDPA," in *Proc. IEEE 4th Broadband Wireless Access Workshop*, 2008.

[16] M. Wrulich and M. Rupp, "Computationally efficient MIMO HSDPA system-level evaluation," 2009, submitted to EURASIP Journal on Wireless Communications and Networking.

[17] Members of 3GPP, "Technical specification group radio access network; spatial channel model for multiple input multiple output (MIMO) simulations," 3GPP, Tech. Rep. 3GPP TS 25.996 Version 7.0.0, Jun. 2007.